Visual Abstract

# Synthesis and characterization of $Fe_2O_3$ nanoparticles reinforced to recycled industrial aluminium scrap & waste aluminium beverage cans for preparing metal matrix nanocomposites

Ganesh R. Chate
*Department of Mechanical Engineering, KLS Gogte Institute of Technology, Affiliated to Visvesvaraya Technological University Belagavi, Karnataka, India*
*ganeshchate@git.edu, https://orcid.org/0000-0001-7735-3566*

Raviraj M. Kulkarni
*Center for Nanoscience and Nanotechnology, KLS Gogte Institute of Technology, Belagavi Affiliated to Visvesvaraya Technological University Belagavi, Karnataka, India.*
*ravirajmk@git.edu, https://orcid.org/0000-0001-6894-6888*

Manjunath Patel G. C.
*Department of Mechanical Engineering, PES Institute of Technology & Management, Shivamogga, Affiliated to Visvesvaraya Technological University Belagavi, Karnataka, India.*
*manju09mpm05@gmail.com, https://orcid.org/0000-0001-9340-7464*

Avinash Lakshmikanthan
*Department of Mechanical Engineering, Nitte Meenakshi Institute of Technology, Bengaluru, Visvesvaraya Technological University, Belagavi 590018, India*
*avinash.laks01@gmail.com, https://orcid.org/0000-0002-6454-2904*

Harsha H. M.
*Department of Mechanical Engineering, GM Institute of Technology, Davanagere, Visvesvaraya Technological University, Belagavi, 590018, India*
*harshahm@gmit.ac.in*

Simran Tophakhane, Nazafali Shaikh, Suman Kongi, Pouravi Iranavar
*Department of Industrial and Production Engineering, KLS Gogte Institute of Technology, Affiliated to Visvesvaraya Technological University Belagavi, Karnataka, India.*
*tsimran01@gmail.com, nazaf22.shaikh@gmail.com, pouravi0496@gmail.com, sumankongi5@gmail.com*

**ABSTRACT.** Increased material demand in all sectors is primarily due to exponential growth in population to fulfill human needs and comforts. Recycling of collected aluminium beverage cans and Al 6061 alloy scraps from industries ensures significant advantages in terms of energy savings with

OPEN ACCESS

**Citation:** Chate, G. R., Kulkarni, R. M., Manjunath, P. G. C., Lakshmikanthan, A.,

reduced environmental problems in fabricating composite parts economically. The iron oxide (α-$Fe_2O_3$) nanoparticles are prepared by precipitation method using ferric chloride and ammonia as a precursor. The prepared nanoparticles were characterized by using Transmission Electron Microscope (TEM), X-Ray Diffraction (XRD) and Fourier Transform Infrared (FTIR). Stir cast processing route ensures uniform mix of reinforcement nanoparticles in matrix material. The prepared nanocomposites (matrix: Al Scrap (90% Scrap Al 6061 alloy + 10% Waste Al can); reinforcement ($Fe_2O_3$): 2%, 4% and 6% wt. of Al matrix) are mechanically characterized for hardness and tensile strengths. It was observed that, increased percent of $Fe_2O_3$ nanoparticles in the metal matrix nanocomposite (MMCs) resulted in significant increase in hardness and tensile strength values. Fractography analysis examined viz. scanning electron microscope (SEM) revealed a ductile failure for as-cast Al scrap followed by brittle failure in Al MMC's.

**KEYWORDS.** Aluminium metal matrix nanocomposites; Ferric oxide nanoparticles; TEM; XRD; FTIR; SEM.

Harsha, H. M., Tophakhane, S., Shaikh, N., Kongi, S., Iranavar, P., Synthesis and characterization of Fe2O3 nanoparticles reinforced to recycled industrial aluminium scrap & waste aluminium beverage cans for preparing metal matrix nanocomposites, Frattura ed Integrità Strutturale, 60 (2022) 229-242.

**Received:** 02.01.2022
**Accepted:** 07.02.2022
**Online first:** 08.02.2022
**Published:** 01.04.2022



## INTRODUCTION

In recent decades, rapid progress in mechanical industries for production of MMCs is primarily to meet the stringent demand (daily production of lakhs of products) that satisfy the human comforts and needs [1, 2]. Aluminium used as the matrix material resulted in excellent blended properties such as strengths (compressive, tensile, impact, fracture), hardness, corrosive and wear resistance [3, 4]. The said properties evolved through aluminium matrix composites are ideal candidature materials that are best suited for automotive and aircraft parts applications [3, 5]. Particles reinforced to MMCs viz. liquid metallurgy route, offered remarkable improvement in stiffness, strength with reduced density and cost [6]. Nanoparticle size reinforcements (i.e., silicon carbide) outperform microscale reinforcements when added to pure steel, in terms of hardness values measured on accumulative roll bonding parts [7, 8]. Similar observations are seen with $Al_2O_3$ particles reinforced in Al 7075 MMCs [9]. In Aluminium MMCs, significant improvement in tribological and mechanical properties was observed with ceramic nanoparticle reinforcements [10], enhanced electric and magnetic permeability was attained with $Fe_3O_4$ -SiC nano particles [11], and multiwall carbon nanotubes resulted in better tensile strengths in magnesium sheets [12]. Therefore, study of different nano-materials and processing methods are of industrial relevance for obtaining better quality composites.

In recent years, use of advanced technology and innovative practices led to rapid progress in developing many liquid metallurgical processing routes for fabricating MMCs [13]. Mass production capability, low cost, simplicity, and uniform dispersion of reinforcement particles in composites ensures, stir casting is an ideal production route compared to other metallurgical route for production of MMCs [14]. Silicon carbide and graphite nanoparticles reinforced to Al 6061 alloy resulted in improved micro-hardness and wear resistance properties [15]. Selection of appropriate proportion of graphite nanoparticles minimizes the negative effects on density and hardness. Aluminium oxide ($Al_2O_3$), and SiC nano particles with magnesium (to improve wettable characteristics) reinforced to Al 7075 alloy resulted in better mechanical behavior coupled with refined grain structures [16]. Ceramic nano-particles reinforced to AlSi9Cu3 alloy improve the flexural strengths in composites [17]. The above literatures confirmed that, the nano-particle reinforcements tend to improve distinguished properties with significant technological benefits.

Magnetic nanoparticles possess unique nanoscale properties (i.e., physical) and their use in magnetic systems are of industrial relevance [18]. Iron oxide (Hematite: α-Fe2O3) treated as most stable and environmentally friendly material used for various applications in inorganic pigments [19], catalysts [20], gas detection sensors [21], energy storage [22], batteries [23], and so on. In addition, α-$Fe_2O_3$ possess applications in multifunctional devices, transducers, actuators and sensors [24, 25]. Although significant applications were found with the use of iron-oxides as nano particles, but their potential use in automotive/aerospace industries requires investigation of mechanical behavior of aluminium MMCs, which are not been focused yet in the literature.

Exponential growth in global population led to increased material demand in all sectors for fulfillment of commercial and basic human needs [26]. Thirteen major elements are treated as high-risk materials in terms of their availability (i.e., generate bottleneck in future) by 2050 [27]. Therefore, sustainable management of aluminium also becomes crucial for extended benefits. Currently, aluminium beverage cans once used are disposed as a landfill material that pollute environments [28]. Recycling waste aluminium cans ensures potential environmental benefits in terms of energy savings, reduction of volume of wastes, and cost-effective [28]. Recycling technology ensures only 5% of energy requirements compared to novel aluminium production (i.e., 8 kg of bauxite ore, 14 KWh of power source, and 4 kg chemicals for production of 1kg pure aluminium) [29, 30]. Not much research efforts being made to fabricate composites with recycled aluminium cans that tested mechanical behaviors suitable for commercial industrial applications.

The present work aims at effective solid waste management of aluminium beverage cans and associated environmental problems in terms of sustainable manufacturing of composites. Al 6061 alloy possess excellent castability and mechanical properties [31]. The recycled waste aluminium beverage cans and Al6061 scraps collected from industries were used as matrix material. The α-$Fe_2O_3$ nanoparticles synthesized by precipitation method (using ferric chloride and ammonia as a precursor) followed by ball milling, is used as the reinforcement materials in MMCs. Nanoparticles were characterized by using TEM, XRD and FTIR. Stir cast processing route is used to prepare the cast and nanocomposite samples. The prepared nanocomposites (matrix: Al Scrap (90% Scrap Al 6061 alloy + 10% Waste Al can); reinforcement: 2%, 4% and 6% wt. of Al matrix) were mechanically characterized for hardness and tensile strength examination.

## EXPERIMENTAL DETAILS: METHODOLOGY, MATERIALS, AND CHARACTERIZATION

### *Methodology*

Fig. 1 shows the methodology followed for the present work. The ferric oxide nano particles are synthesized by precipitation method. The synthesized nanoparticles were used as reinforcements, which are then characterized with the help of TEM, FTIR, and XRD. The Al6061 scrap and aluminium beverage cans were collected, and are used as a matrix material for preparing the MMCs. Stir casting process ensures uniform dispersion of reinforcements in matrix material and are used to prepare the nanocomposites. The nanocomposites prepared with different wt. % of $Fe_2O_3$ nano particles (2, 4, and 6%) reinforcements. Three replicates are prepared for each percent reinforcements in nanocomposites. The average values (27 BHN values) of Brinell hardness number and 3 tensile strengths (ultimate tensile strength and yield strength) of samples is recorded and are used for analysis. The chemical compositions of casting samples Al scraps (90% Scrap Al 6061 alloy + 10% Waste Al can) were determined subjected to optical emission spectroscopy.

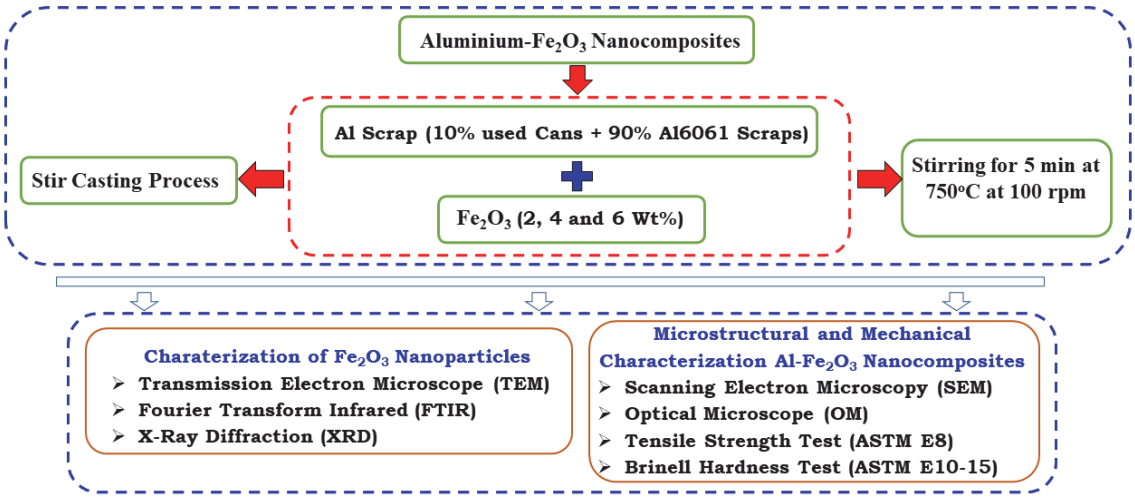


Figure 1: Flowchart illustrate the experimental details of methodology, materials and their characterization.

### *Synthesis of $Fe_2O_3$ Nanoparticles*

Fig. 2 show the illustration of synthesis of $Fe_2O_3$ nanoparticles, and are explained as follows. Precipitation method is used for synthesis of $Fe_2O_3$ nanoparticles. Initially, a pre-determined quantity of Ferric Chloride ($FeCl_3$) was taken in a conical flask which was later converted to a liquid solution using distilled water. Approximately 5 ml of HCl was added to the

solution to remove the excess of Chlorine (present if any). The diluted ammonia was first filled into the burette and titrated with the solution. The solution was stirred continuously with the help of mechanical stirrer. This process was repeated till it ensures thick solution. Later, the titrated solution was allowed to settle for a few hours. The nanoparticles are settled at the bottom of the beaker. The water is then removed and replaced with fresh distilled water. This process ensures removal of excess chlorine (present if any). After cleaning the solution repeatedly for several times, the beaker is then heated in a fume hood to remove excess moisture and form a paste. This paste is removed in a crucible and then heated in a furnace. The paste is converted into agglomerated nanoparticles. The particles are later finely crushed, so as to obtain a fine powder in a crusher. The density of the prepared nanoparticles was found equal to 5.2 gm/cm$^3$. The chemical reaction between ferric chloride and ammonium hydroxide takes place which could results in the formation of ferric oxide and ammonium chloride. Excess water is then removed. The solution is washed several times to remove the Ammonium Chloride and finally the nanoparticles are obtained.

$$2FeCl_3 + 6NH_4OH \rightarrow Fe_2O_3.3H_2O + 6NH_4Cl \quad (1)$$

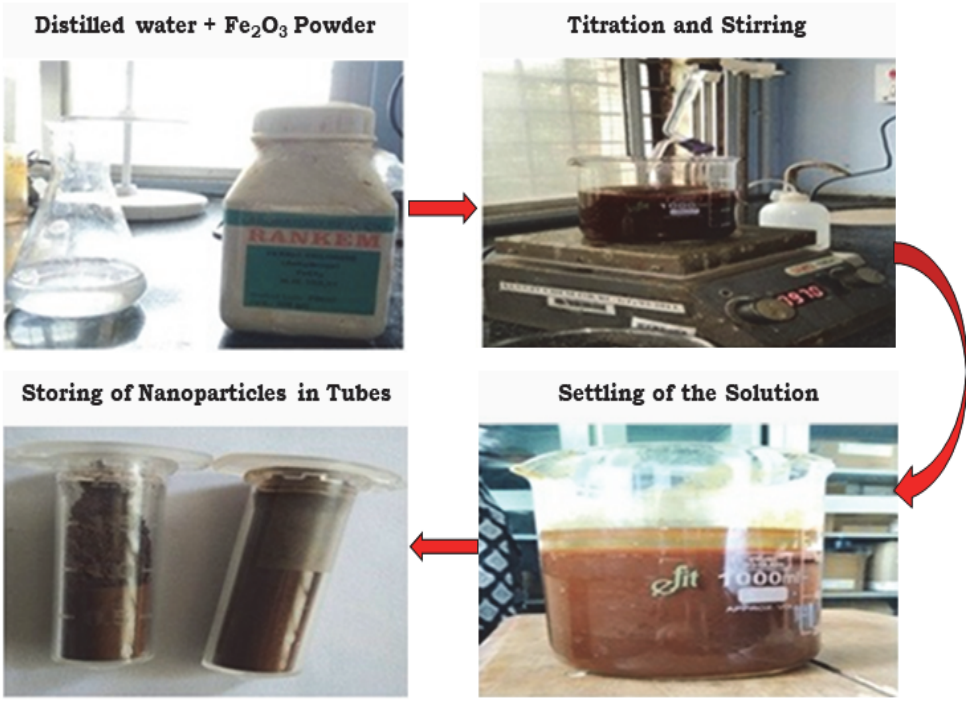


Figure 2: Schematic of synthesis of iron oxide nanoparticles.

*Characterization of Nanoparticles*

The prepared nanoparticles were sent to STIC India, Kochi (Kerala, India) for performing different characterization. The nanoparticles are characterized with the help of TEM, FTIR and XRD.

TEM Image of iron oxide nano-particles is depicted in Fig. 3. It confirms from the TEM image that the diameter of $Fe_2O_3$ nanoparticles is found approximately equal to 50-60 nm. Note that, the nanoparticles are seen to have oval shape. There were no bright spots in the form of concentric circles in the image, hence $Fe_2O_3$ nano particles are crystalline in nature. The Fourier Transform Infrared Spectroscopy image of $Fe_2O_3$ nanoparticles is shown in Fig. 4. The image of FTIR consists of four peak points. The spectrum of gamma $Fe_2O_3$ nanoparticles show the characteristic broadband value of 3430.42 cm$^{-1}$, which is primarily due to the stretching vibration of O-H bond. The two intense Infrared bands i.e., 540 cm$^{-1}$ and 475.15 cm$^{-1}$ are typical for ferrihydrite of gamma $Fe_2O_3$ nanoparticles. The bending vibrations of O-H group are at 1628.31 cm$^{-1}$. X-ray peaks and associated planes are observed at 24.176$^0$ is (0 1 2), 33.192$^0$ is (1 0 4), 36.668$^0$ is (1 1 0), 40.904$^0$ is (1 1 3), 49.614$^0$ is (0 2 4), 54.123$^0$ is (1 1 6), 62.495$^0$ is (2 1 4), 64.060$^0$ is (3 0 0) and 72.006$^0$ is (1 0 1) of α-$Fe_2O_3$, respectively. XRD pattern of synthesized nanoparticles confirms that the $Fe_2O_3$ is in α-phase. Note that, all the X-ray peaks are indexed to JCPDS card no. 89-0598. The XRD graph of nanoparticles are shown in Fig. 5.

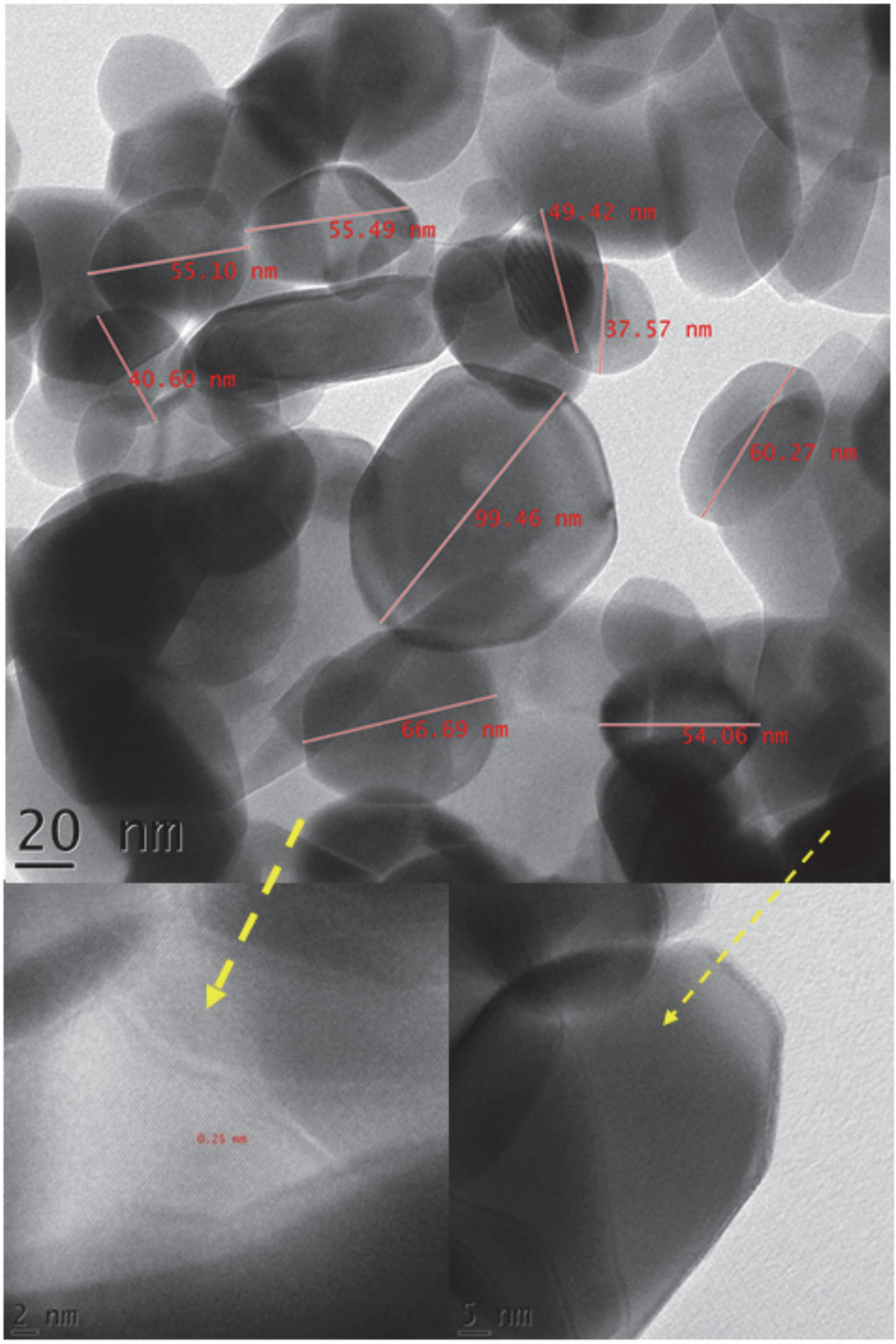


Figure 3: TEM characterization of iron oxide nanoparticles

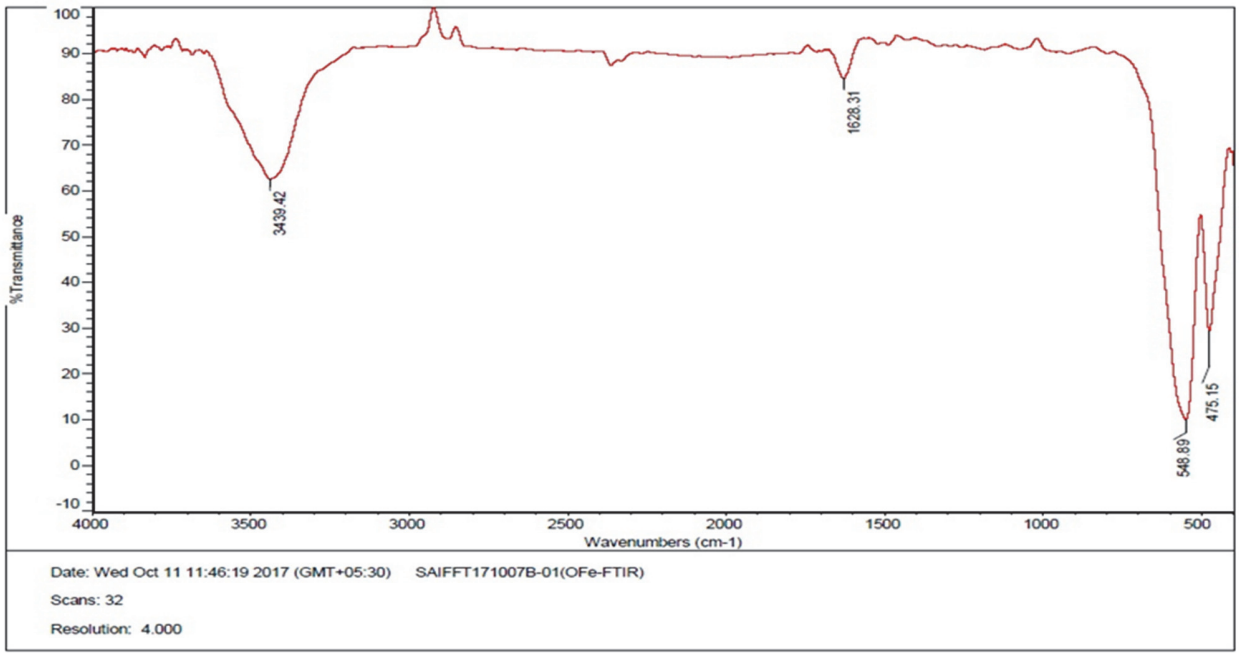


Figure 4: FTIR characterization of iron oxide nanoparticles.

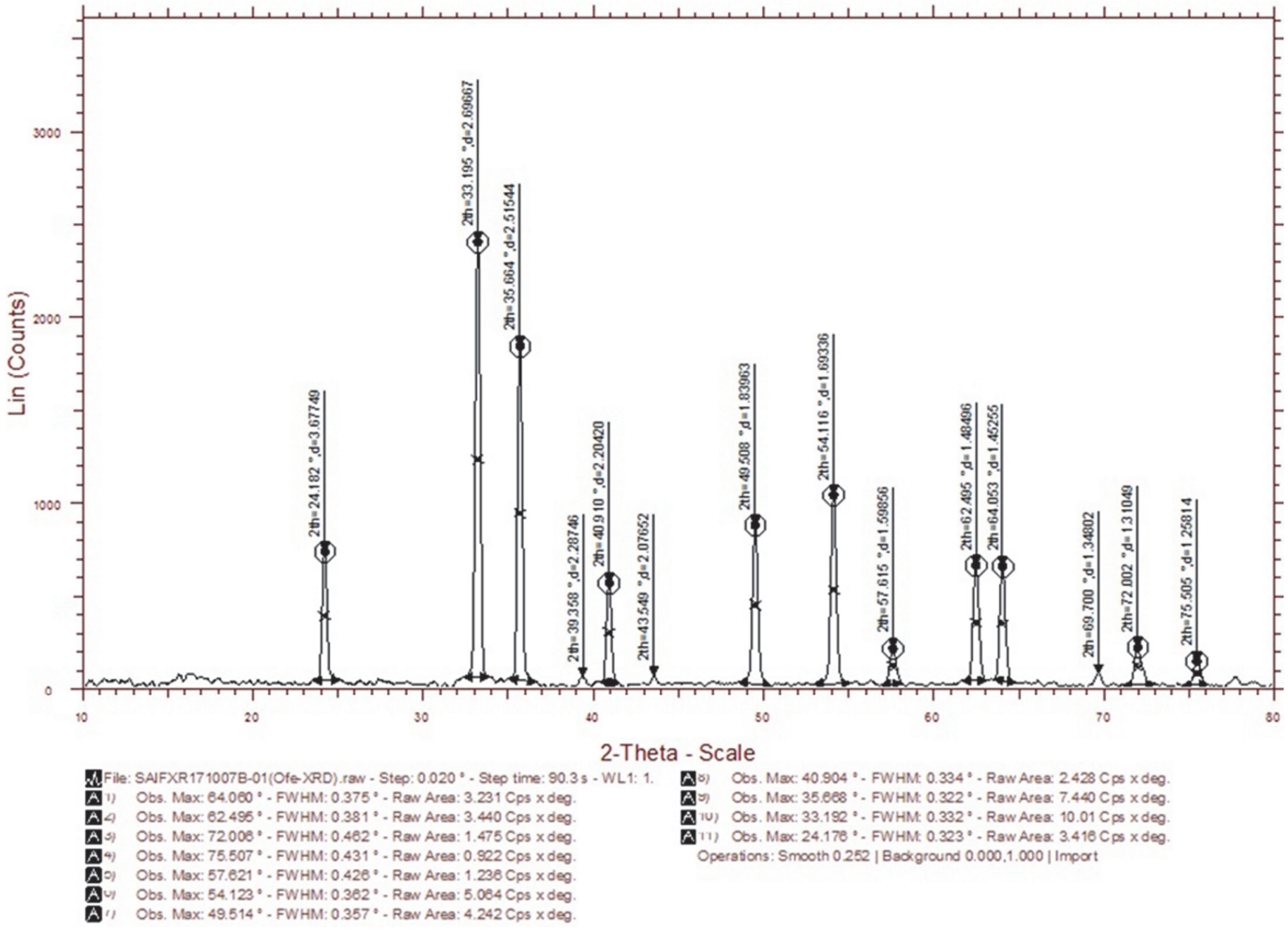


Figure 5: XRD characterization of iron oxide nanoparticles.

*Stir Casting Method*

The prepared nanoparticles were used as the reinforcement material with varying percentage (2%,4% and 6% weight of $Fe_2O_3$) in the molten aluminium scrap metal (90% Scrap Al 6061 alloy + 10% Waste Al can) matrix in a crucible of stir casting set-up. The crucible is placed inside a bucket which is lined by bentonite (clay) that ensures uniform transfer of heat. The stir casting set-up was fabricated using bevel gears with an adjustable blade height maintained at a speed ratio equal to 1.6. The stirring was carried out mechanically at a speed rate of 100 rpm. The degassing capsules (hexachloroethane: $C_2Cl_6$) ensures removal of absorbed or generated gasses in the prepared molten matrix. The prepared molten metal is poured at 750°C to the preheated (say 200 °C) mold possessing cavity dimensions of 25 mm diameter and 75 mm height. After ensuring complete solidification (allowed to solidify at room temperature) of nanocomposite samples, machining (turning and facing) has been done. After slicing the specimen to three different heights, hardness measurement was taken on the nanocomposite samples at different locations.

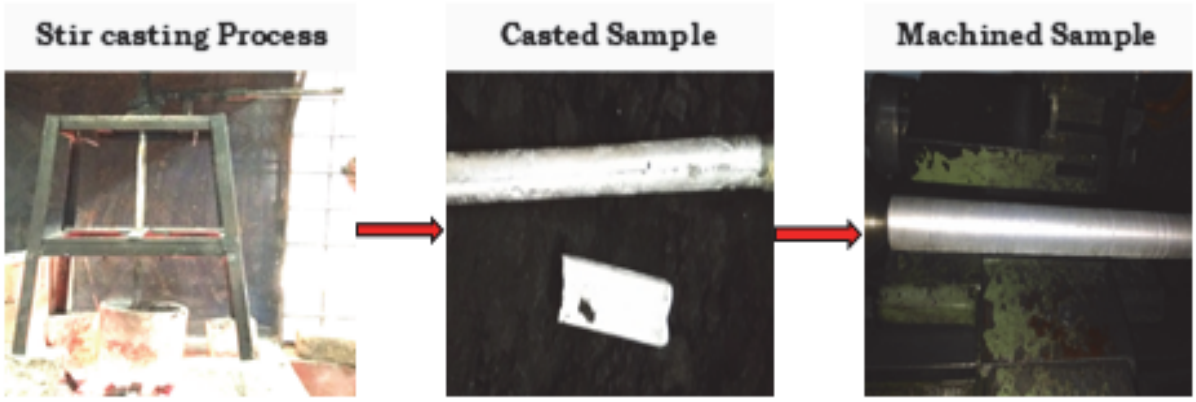


Figure 6: Process flow of preparing MMCs

The spectral analysis of the as-cast aluminium MMCs are carried out and the composition of the samples are given in Tab. 1.

| Elements | Si | Fe | Cu | Mn | Mg | Cr | Ni | Zn | Ti | V | Other (P, Sn, Sr, Be) | Al |
|---|---|---|---|---|---|---|---|---|---|---|---|---|
| Composition (%) | 1.13 | 0.59 | 0.36 | 0.82 | 0.11 | 0.02 | 0.01 | 0.15 | 0.02 | 0.012 | 0.058 | 96.72 |

Table 1: The chemical composition of as-cast aluminium MMCs by optical emission Spectroscopy analysis

*Hardness Test and Microstructural Characterization*

Brinell hardness tester (ball indenter: 2.5 mm and load of 187.5 kg) was carried out to record the hardness values of the nanocomposite samples. The test specimens are prepared according to ASTM E10-15 reference standard. Hardness measurements are carried out at three different locations (top, middle and end) possessing the average values (9 measurements on each sample and 3 replicates) of 27 BHN readings on the nanocomposite samples are recorded and performed analysis. The computation of BHN values is recorded using Eqn. 2.

$$BHN = \frac{2P}{\Pi D\left(D - \sqrt{\left(D^2 - d^2\right)}\right)} \tag{2}$$

Term, P is the load applied by ball (187.5 kg). D refers to diameter of the ball indenter equal to 2.5 mm and term d be the measured indentation diameter, respectively. Microstructural analysis was carried out subjected to optical microscopy. Prior to the analysis, the samples are polished to obtain a mirror surface (without scratches or dents) as per the standard procedure.

## RESULTS AND DISCUSSION

### *Hardness characterization*

The BHN correspond to casting (as-cast) and nanocomposites (at different weight proportions of nanoparticles) are presented in Tab. 2. Compared to cast (no reinforcements) sample, the nanocomposite samples exhibited the higher hardness values. Similar observations with enhanced properties (mechanical, microstructure and tribological) are reported with other reinforcement particles (TiC, CNT, graphene, fly-ash etc.) dispersed to Al alloy [32-34]. This could be attributed to the presence of reinforcement particles hinders the dendritic growth, serves as nucleation sites at many distinct locations results in refinement in the grain structure [35]. Increase in hardness values are observed with proportionate increase in weight percent of α-$Fe_2O_3$ nano particles (refer Fig. 7). Maximum hardness values are obtained for the nanocomposite sample with 6% wt. $Fe_2O_3$ nano particles. This might be due to the occupancy of $Fe_2O_3$ nanoparticles on larger surface area in aluminium metal matrix and iron oxide being harder as compared to aluminium. The resistance offered by the nanoparticles (that are dispersed uniformly throughout the matrix) for indentation also increases with an increase in the amount of $Fe_2O_3$ and this occurs due to hard reinforcements compared to soft Aluminium metal matrix. The hardness value tends to show no appreciable improvement beyond 6% wt. during examination. This could be probably due to the agglomeration formation, and affected fluid flow characteristics (viscosity, and surface tension) [36].

| Samples | Al Scrap | Al Scrap + 2% $Fe_2O_3$ particles | Al Scrap + 4% $Fe_2O_3$ particles | Al Scrap + 6% $Fe_2O_3$ particles |
|---|---|---|---|---|
| BHN | 45.12 | 48.26 | 68.54 | 79.49 |
| Density ($g/cm^3$) | 2.609 | 2.702 | 2.744 | 2.808 |

Table 2: The BHN values of cast and composite samples

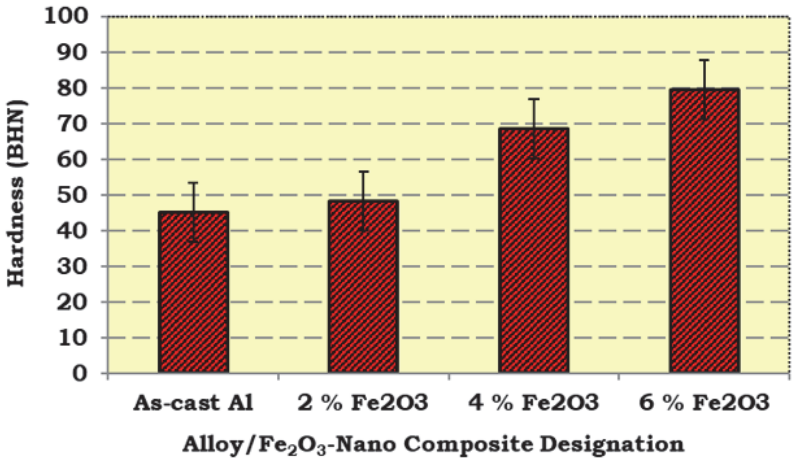


Figure 7: Hardness values of cast and nanocomposite samples

### *Microstructural Analysis using Optical Microscopes*

Optical microscope examinations are performed on the cast and nanocomposite samples. The microstructure obtained by optical microscope is shown in Fig. 8. As the amount of $Fe_2O_3$ reinforcement particles increases the density also increased, this occurs due to the particle reinforcements has higher density compared to metal matrix [37, 38]. The increase in hardness with increase in reinforcement may be due to the fact that higher volume occupancy of $Fe_2O_3$ nanoparticles [39]. The melting point of $Fe_2O_3$ nanoparticles is more as compared to aluminium metal matrix and hence the liquid aluminium coats the solid $Fe_2O_3$ nanoparticles which are harder, and this might have increased the hardness in nanocomposites. The $Fe_2O_3$ nanoparticles are not allowed to settle at the bottom of crucible as molten metal is stirred continuously before pouring. Pouring is done immediately during the whirl effect of liquid, thus ensuring that $Fe_2O_3$ nanoparticles will not settle at the bottom and distribute evenly throughout the melt. Therefore, agglomeration of nanoparticles was not seen in the nanocomposite samples (refer to Fig. 8). This can be clearly seen in the microstructure, wherein the reinforcement particle percent increases with increased proportion in the nanocomposites (refer to Fig. 8). During casting $Fe_2O_3$ nanoparticles assist for nucleation.

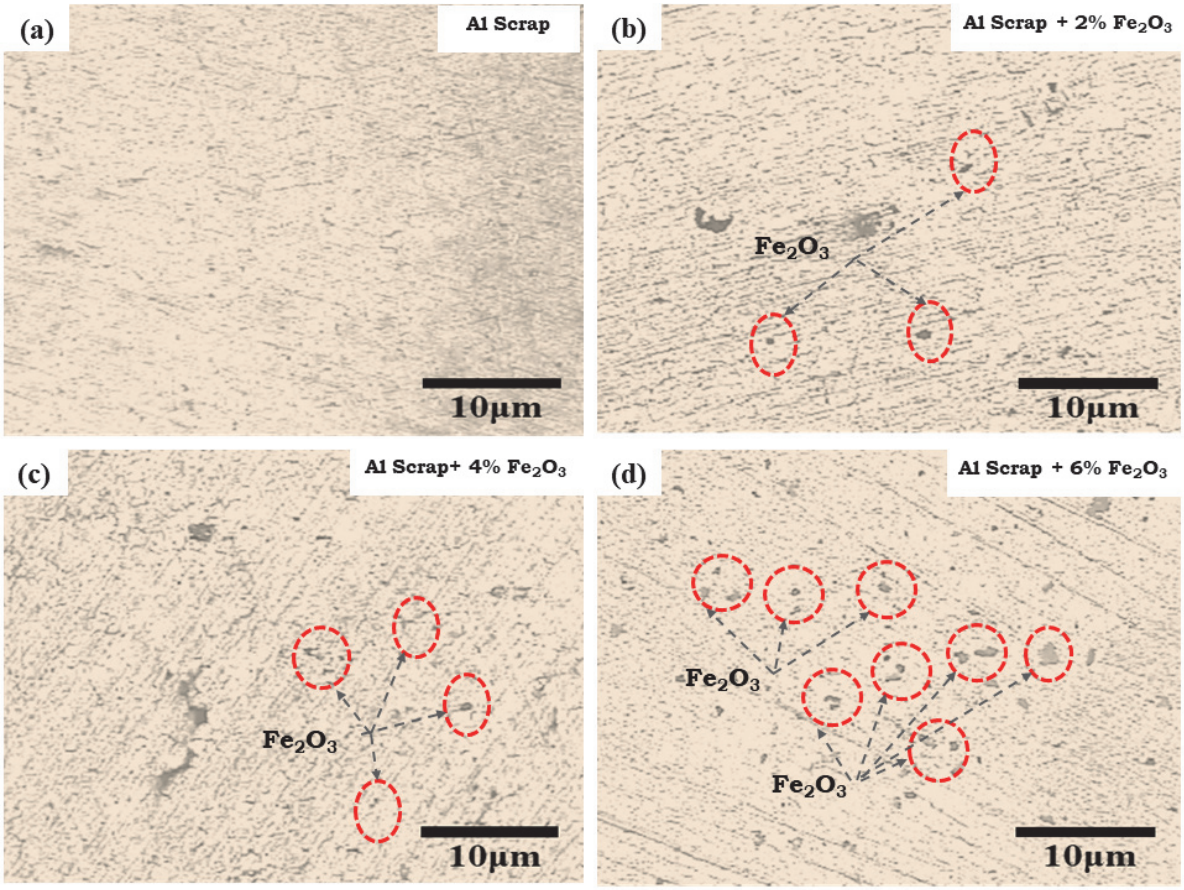


Figure 8: Optical Micrographs of cast and nanocomposite samples

*Fractographic studies*

The tensile test of Al6061 scrap MMC's reinforced with α-$Fe_2O_3$ nanoparticles was conducted as per ASTM E8 standards at room temperature. The dimensions of tensile test samples are given in Fig. 9. The results were based on an average of three readings conducted at a strain rate of 0.2 mm/s in Universal Testing Machine.

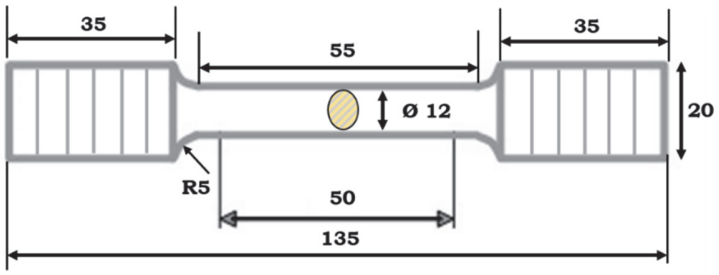


Figure 9: Tensile test sample dimensions.

Fig. 10 depicts the variation of the tensile strength (UTS and YS) corresponds to different weight percentage of α-$Fe_2O_3$ nanoparticles. Fig. 10 depicts that increased percent of reinforcement of $Fe_2O_3$ showed proportionate increase in YS and UTS. It was observed that, the strength (UTS and YS) concurrently enhanced by 17 % and 24% as the wt. % of $Fe_2O_3$ increased from 0 to 6 wt.%. in contrast with Al6061 alloy. The load vs. displacement curves of the tested samples is presented in Fig. 11. The mechanical properties (hardness, strength, etc.) of the composites are directly or indirectly controlled by the composition of the reinforcements [40] may assist in effective load transfer between the matrix and reinforcement, leading to improvement in strength. Similar observations were made by several researchers [32, 41]. From Tab. 3, it is observed that as the wt. % of $Fe_2O_3$ particles increased from 0 to 6 wt.% there is a reduction in ductility by 34 % (from 7.58 – 5.01)

compared to Al6061 alloy, which is a very general trend confronted drawback in MMC's [42]. Titanium carbide reinforcement to AA6061 alloy resulted in reduced ductility by 44.1% (from 9.2 to 5.14) compared to Al6061 alloy useful for various engineering applications [43]. Al6061 MMCs reinforced with various materials (SiC, $Al_2O_3$, $B_4C$, Gr) possess similar ductility ranges and are potentially used in production of various automobile and aerospace parts [44-45]. The decrease in ductility may be attributed to a hard reinforcement phase, which leads to the initiation of crack and enhanced fragility effect owing to the local concentration of stress spots at the reinforcement-matrix interface [46-47].

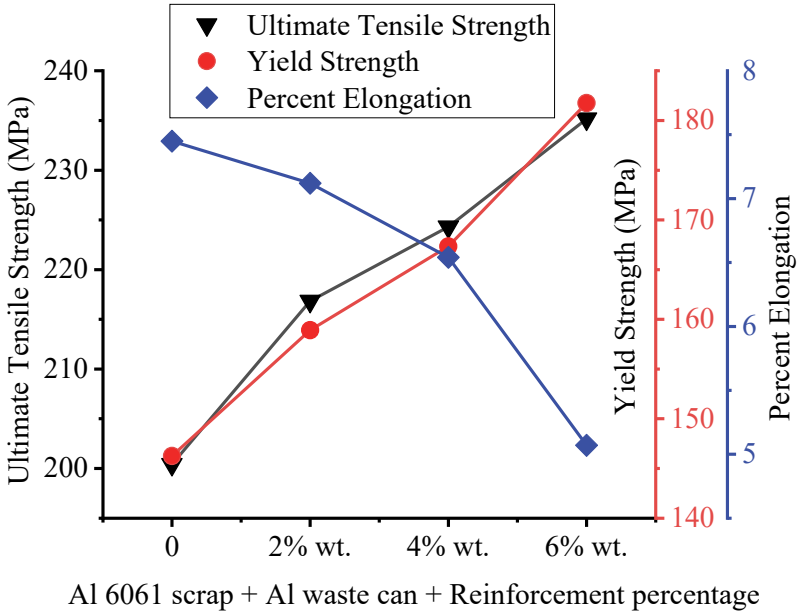


Figure 10: Tensile strength characterization of cast and nanocomposite samples.

| Tests | Al Scrap | Al Scrap + 2% $Fe_2O_3$ particles | Al Scrap + 4% $Fe_2O_3$ particles | Al Scrap + 6% $Fe_2O_3$ particles |
|---|---|---|---|---|
| UTS (MPa) | 200.42 | 216.84 | 224.31 | 235.16 |
| Percent increase in UTS compared to Al Scrap | | 8.19 | 11.91 | 17.33 |
| YS (MPa) | 146.26 | 158.91 | 167.34 | 181.75 |
| Percent increase in YS compared to Al Scrap | | 8.64 | 14.41 | 24.26 |
| Ductility | 7.58 | 7.18 | 6.54 | 5.01 |
| Percent decrease in ductility compared to Al Scrap | | 5.28 | 13.72 | 34 |

Table 3: The tensile strength values of cast and composite samples.

Fig. 12 depicts the fractography of Al6061 MMC's reinforced with α-$Fe_2O_3$ nanoparticles. Fig. 12(a-d), numbering 1, 2, 3, 4, 5 illustrates Al grains (α), voids, particle pull-out region, stream-like pattern, and cleavage façade. Fig. 12(a) shows as-cast Al 6061 scrap. From Fig. 12(a), many uneven small-sized ductile dimples are observed, which clearly depicts the mode of fracture is ductile in nature [48]. Fig. 12(b) shows as-cast 6061 scrap + 2% wt. $Fe_2O_3$. Fig. 12(b) shows clearly the particle pull-out regions at various sites. In addition, uneven tear edges along with cavities and cleavage façade, are observed which indicates the brittle failure in MMC's. Figs. 12(c) and (d) show 4% wt. of $Fe_2O_3$ and 6% wt. of $Fe_2O_3$ nanoparticles reinforced with as-cast Al 6061 scrap. These figures display similar characteristics to that of Fig. 12(b). An increase in α-$Fe_2O_3$ content in the MMC's resulted in a brittle fracture combined with evidently distinct dimples, as shown in Figs. 12(c) and (d). Overall, it was noted that the number of particles (i.e., fractured or unbonded) occur on the rupture surface increases with increased reinforced particles, as shown in Figs. 12(b), (c), and (d). Similar observations were made by other researchers [49-51].

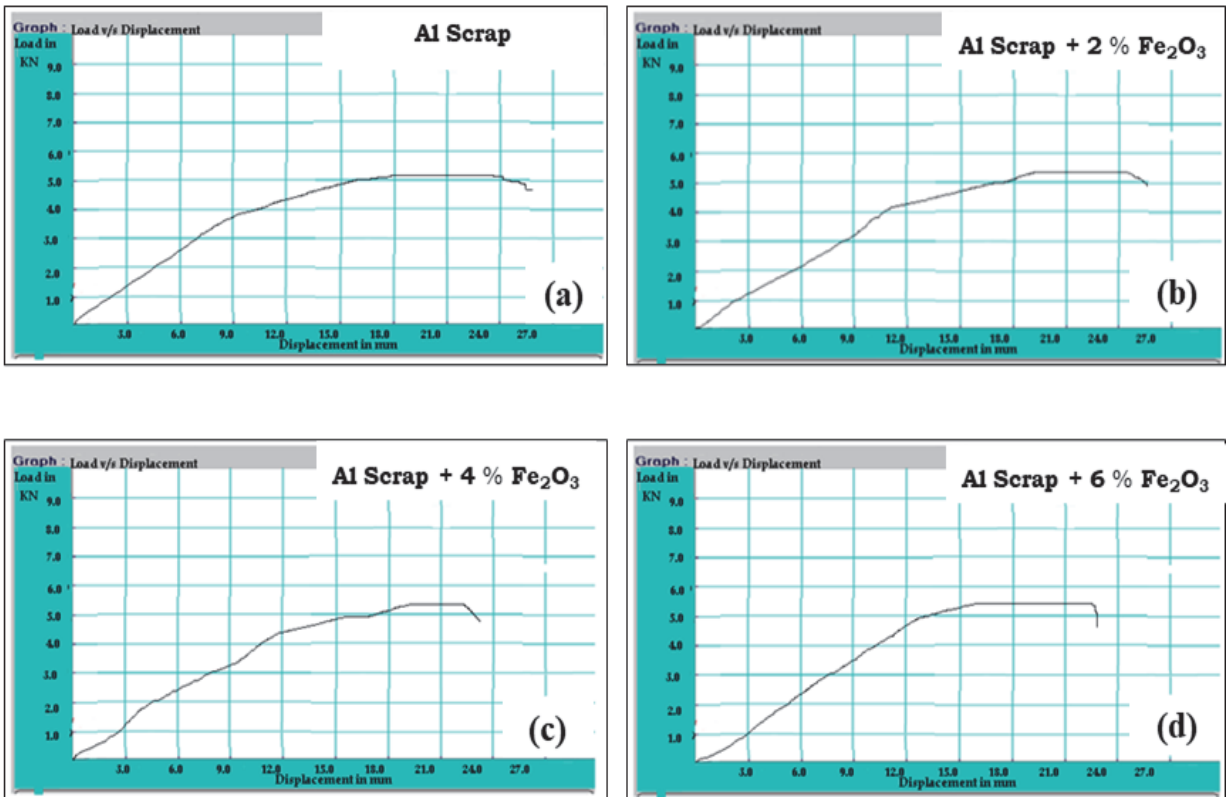


Figure 11: Load vs. Displacement curves of: a) Al Scrap, b) Al Scrap + 2% $Fe_2O_3$, c) Al Scrap + 4% $Fe_2O_3$, d) Al Scrap + 6% $Fe_2O_3$,

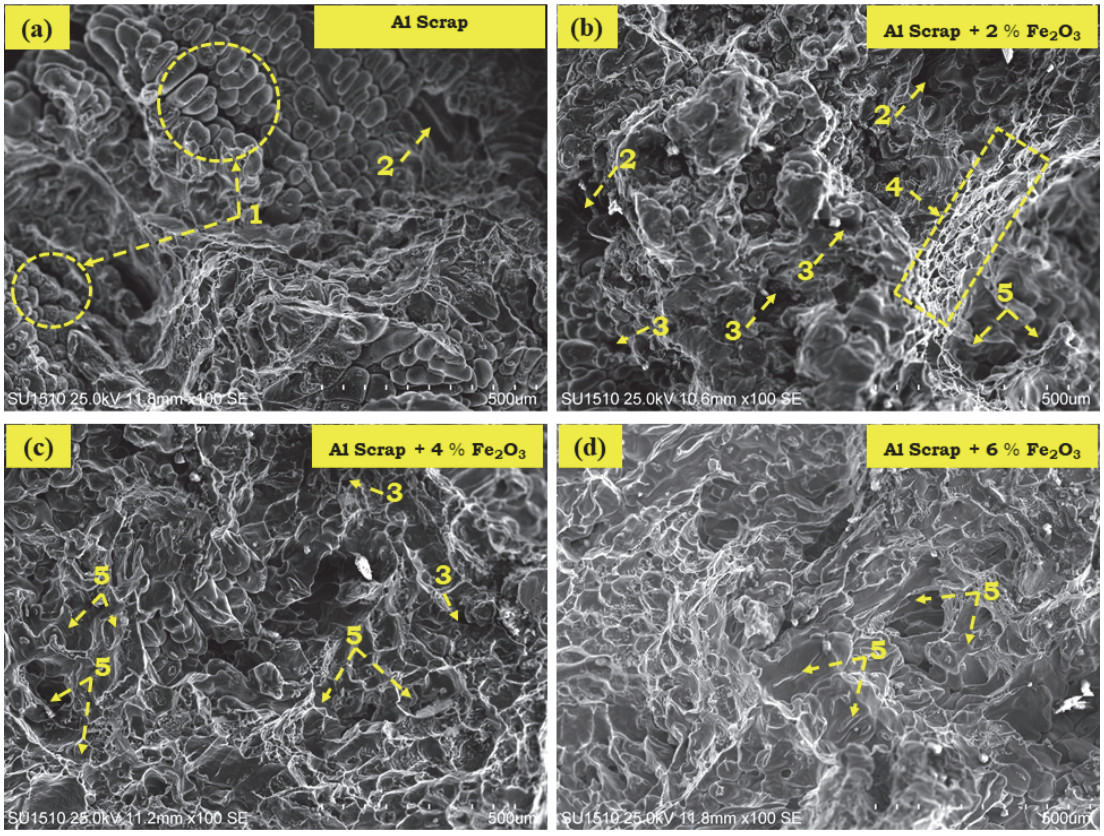


Figure 12: Fractography of Al6061 scrap MMC's reinforced with α-$Fe_2O_3$ nanoparticles.

## CONCLUSIONS

The following conclusions were drawn based on the current research work

1. The iron oxide nanoparticles ($\alpha$-$Fe_2O_3$) were prepared successfully to a particle size of 50-60nm, by precipitation method using ferric chloride and ammonia as a precursor.
2. The Al MMC's was successfully developed by liquid metallurgy route using Al 6061 (90% weight) industrial scrap and waste aluminium beverage cans (10% weight) as a matrix, and $\alpha$-$Fe_2O_3$ as reinforcement.
3. The hardness and tensile strength of the nanocomposite increased with increased proportion of $\alpha$-$Fe_2O_3$ nanoparticles. This occurs due to more volume occupancy of nanoparticles which consists of iron oxide which is harder compared to that of aluminium.
4. Optical micrographs of Al 6061 MMC's revealed a fairly distribution of $\alpha$-$Fe_2O_3$ nanoparticles in the matrix with minimal porosity.
5. Fractography analysis indicated a ductile failure in the case of as-cast Al6061 scrap, whereas brittle failure in Al 6061 MMC's
6. The obtained results ensure the waste scrap collected from industries and aluminium beverage cans possess greater potential to yield higher hardness and density in the nanocomposites. Therefore, these nanocomposites can be used for production in industrial scale suitable for mechanical applications.

## REFERENCES

[1] Manjunath Naik H R, Manjunath L H, Vishwanath Koti, Avinash Lakshmikanthan, Praveennath G Koppad, Sampath kumaran P. (2021), Al/Graphene/CNT Hybrid Composites: Hardness and Sliding Wear Studies, FME Transactions (2021) 49, pp. 414-421. DOI: 10.5937/fme2102414N.

[2] Reddy, P.V., Kumar, G.S., Krishnudu, D.M. and Rao, H.R. (2020). Mechanical and wear performances of aluminium-based metal matrix composites: a review. J. Bio- Tribo-Corros. 6, pp. 1-16. DOI: 10.1007/s40735-020-00379-2.

[3] Ononiwu, N.H., Akinlabi, E.T. and Ozoegwu, C.G. (2021). Optimization techniques applied to machinability studies for turning aluminium metal matrix composites: A literature review, Mater. Today: Proc., 44, pp. 1124-1129. DOI: 10.1016/j.matpr.2020.11.228.

[4] Doddamani, S., Wang, C., Jinnah, M.S.M. and ArefinKowser, M. (2021). Fracture analysis of AA6061-graphite composite for the application of helicopter rotor blade, Frat. Integrita Strutt., 58, pp. 191-201. DOI: 10.3221/IGF-ESIS.58.14.

[5] Samal, P., Vundavilli, P.R., Meher, A. and Mahapatra, M.M. (2020). Recent progress in aluminum metal matrix composites: A review on processing, mechanical and wear properties, J. Manuf. Process., 59, pp. 131-152. DOI: 10.1016/j.jmapro.2020.09.010.

[6] Adithya Parthasarathy, Avinash L, Varun Kumar KN, Basavaraj Sajjan, Varun S (2017). Fabrication and Characterization of Al-0.4%Si-0.5%Mg - SiCp using Permanent Mould Casting Technique" Applied Mechanics and Materials, Trans Tech Publications, Switzerland, ISSN: 1662-7482, 867, pp 34-40, DOI: 10.4028/www.scientific.net/AMM.867.34

[7] Jamaati, R., Toroghinejad, M.R., Edris, H. and Salmani, M.R. (2014). Comparison of microparticles and nanoparticles effects on the microstructure and mechanical properties of steel-based composite and nanocomposite fabricated via accumulative roll bonding process, Mater. Des. (1980-2015), 56, pp. 359-367. DOI: 10.1016/j.matdes.2013.11.049.

[8] Casati, R. and Vedani, M. (2014). Metal matrix composites reinforced by nano-particles—a review, Metals, 4(1), pp. 65-83. DOI: 10.3390/met4010065.

[9] Ravikumar, M., Reddappa, H.N., Suresh, R., Babu, E.R. and Nagaraja, C.R. (2021). Study on micro-nano sized Al2O3 particles on mechanical, wear and fracture behavior of Al7075 Metal Matrix Composites, Frat. Integrita Strutt., 15(58), pp. 166-178; DOI: 10.3221/IGF-ESIS.58.12.

[10] Das, S., Chandrasekaran, M., Samanta, S., Kayaroganam, P. and Davim, P. (2019). Fabrication and tribological study of AA6061 hybrid metal matrix composites reinforced with SiC/B4C nanoparticles, Ind. Lubr. Tribol. 71(1), pp. 83-93. DOI: 10.1108/ILT-05-2018-0166.

[11] Ashrafi, N., Ariff, A.H.M., Sarraf, M., Sulaiman, S. and Hong, T.S. (2021). Microstructural, thermal, electrical, and magnetic properties of optimized $Fe_3O_4$–SiC hybrid nano filler reinforced aluminium matrix composite, Mater. Chem. Phys., 258, pp. 123895. DOI: 10.1016/j.matchemphys.2020.123895.

[12] Merino, C.A.I., Sillas, J.L., Meza, J.M. and Ramirez, J.H. (2017). Metal matrix composites reinforced with carbon nanotubes by an alternative technique, J. Alloys Compd., 707, pp. 257-263. DOI: 10.1016/j.jallcom.2016.11.348.
[13] Senthil, S., Raguraman, M. and Manalan, D.T. (2021). Manufacturing processes & recent applications of aluminium metal matrix composite materials: A review, Mater. Today: Proc., 45, pp. 5934-5938. DOI: 10.1016/j.matpr.2020.08.792.
[14] Ramanathan, A., Krishnan, P.K. and Muraliraja, R. (2019). A review on the production of metal matrix composites through stir casting–Furnace design, properties, challenges, and research opportunities, J. Manuf. Process., 42, pp. 213-245. DOI: 10.1016/j.jmapro.2019.04.017.
[15] Reddy, A.P., Krishna, P.V. and Rao, R.N. (2019). Tribological behaviour of Al6061–2SiC-xGr hybrid metal matrix nanocomposites fabricated through ultrasonically assisted stir casting technique, Silicon, 11(6), pp. 2853-2871. DOI: 10.1007/s12633-019-0072-9.
[16] Suresh, S., Gowd, G.H., and Kumar, M.D. (2019). Mechanical properties of AA 7075/Al 2 O 3/SiC nano-metal matrix composites by stir-casting method, J. Inst. Eng. India Ser. D., 100(1), pp. 43-53. DOI: 10.1007/s40033-019-00178-1.
[17] Ünal, T.G. and Diler, E.A. (2018). Properties of AlSi9Cu3 metal matrix micro and nano composites produced via stir casting, Open Chem. 16(1), pp. 726-731. DOI: 10.1515/chem-2018-0079.
[18] Farahmandjou, M. and Soflaee, F. (2015). Synthesis and characterization of α-Fe2O3 nanoparticles by simple co-precipitation method, Phys. Chem. Res., 3(3), pp. 191-196.
[19] Lassoued, A., Dkhil, B., Gadri, A. and Ammar, S. (2017). Control of the shape and size of iron oxide (α-Fe2O3) nanoparticles synthesized through the chemical precipitation method, Results Phys., 7, pp. 3007-3015. DOI: 10.1016/j.rinp.2017.07.066.
[20] Li, F., Wang, X., Pan, H., Li, Q. and Yang, J. (2019). Preparation of disk-like α-Fe2O3 nanoparticles and their catalytic effect on extra heavy crude oil upgrading, Fuel, 251, pp. 644-650. DOI: 10.1016/j.fuel.2019.04.048.
[21] Choudhary, S., Annapoorni, S. and Malik, R. (2021). Facile strategy to synthesize donut-shaped α-Fe2O3 nanoparticles for enhanced LPG detection, Sens. Actuators B: Chem., 334, pp. 129668. DOI: 10.1016/j.snb.2021.129668.
[22] Orisekeh, K., Singh, B., Olanrewaju, Y., Kigozi, M., Ihekweme, G., Umar, S. and Soboyejo, W.O. (2021). Processing of $\alpha$-$Fe_2O_3$ Nanoparticles on Activated Carbon Cloth as Binder-Free Electrode Material for Supercapacitor Energy Storage, J. Energy Storage., 33, pp. 102042. DOI: 10.1016/j.est.2020.102042.
[23] Wu, W., Wei, Y., Chen, H., Wei, K., Li, Z., He, J. and Yang, H. (2021). In-situ encapsulation of α-Fe2O3 nanoparticles into ZnFe2O4 micro-sized capsules as high-performance lithium-ion battery anodes, J. Mater. Sci. Technol., 75, pp. 110-117. DOI: 10.1016/j.jmst.2020.10.039.
[24] Katundi, D., Ferreira, L.P., Bayraktar, E., Miskioglu, I., Robert, M.H. (2017). Design of magnetic aluminium (A356) based composites through combined method of sinter + forging. SEM, Mech. Composite Multi-funct. Mater. 6, pp. 89–101. DOI: 10.1007/978-3-319-63408-1.
[25] Ferreira, L.P., Bayraktar, E., Miskioglu, I. and Robert, M.H. (2019). Design of Magnetic Aluminium (AA356) Composites (Amcs) Reinforced with Nano $Fe_3O_4$, and Recycled Nickel: Copper Particles, In Mechanics of Composite, Hybrid and Multifunctional Materials, 5, pp. 93-100. DOI: 10.1007/978-3-319-95510-0_12.
[26] Valero, A., Valero, A., Calvo, G., Ortego, A., Ascaso, S. and Palacios, J.L. (2018). Global material requirements for the energy transition. An exergy flow analysis of decarbonisation pathways, Energy, 159, pp. 1175-1184. DOI: 10.1016/j.energy.2018.06.149.
[27] Valero, A., Valero, A., Calvo, G. and Ortego, A. (2018b). Material bottlenecks in the future development of green technologies, Renew. Sust. Energ. Rev., 93, pp. 178-200. DOI: 10.1016/j.rser.2018.05.041.
[28] Bin Mokaizh, A.A., and Shariffuddin, J.H.B.H. (2021). Manufacturing of Nanoalumina by Recycling of Aluminium Cans Waste, A. S. H. Makhlouf and G. A. M. Ali (eds.), Waste Recycling Technologies for Nanomaterials Manufacturing, pp. 851-870. DOI: 10.1007/978-3-030-68031-2_30.
[29] Verran, G.O., and Kurzawa, U. (2008). An experimental study of aluminum can recycling using fusion in induction furnace, Resour Conserv Recycl, 52(5), pp. 731-736. DOI: 10.1016/j.resconrec.2007.10.001.
[30] Liu, W., Niu, T., Yang, J., Wang, Y., Hu, S., Dong, Y., and Xu, H. (2011). Preparation of micron-sized alumina powders from aluminium beverage can by means of sol-gel process, Micro Nano Lett., 6(10), pp. 852-854. DOI: 10.1049/mnl.2011.0491.
[31] James, S.J., Ganesan, M., Santhamoorthy, P. and Kuppan, P. (2018). Development of hybrid aluminium metal matrix composite and study of property, Mater. Today: Proc., 5(5), pp. 13048-13054. DOI: 10.1016/j.matpr.2018.02.291
[32] Vinayaka, N., Lakshmikanthan, A., Manjunath Patel, G.C. and Pon, C. (2021). Mechanical, Microstructure and Wear properties of Al 6113 Fly Ash reinforced Composites: Comparison of as-cast and Heat-treated Conditions. Advances in Materials and Processing Technologies, DOI: 10.1080/2374068X.2021.1927649.

[33] Naik, H.R., Manjunath, L.H., Malik, V., Patel, G.C.M., Saxena, K.K. and Lakshmikanthan, A. (2021). Effect of microstructure, mechanical and wear on Al-CNTs/graphene hybrid MMC'S, Advances in Materials and Processing Technologies, pp. 1-14. DOI: 10.1080/2374068X.2021.1927646.
[34] Raviraj, M.S., Patel, G.C.M. and Sharanaprabhu, C.M. (2021). Study of geometric parameters and TiC reinforcements in aluminium metal matrix composite on fracture toughness using Taguchi method. Mater. Today: Proc.,46(8), pp. 8900-8904. DOI: 10.1016/j.matpr.2021.05.358.
[35] Swamy, P.K., Mylaraiah, S., Patel G.C.M., Lakshmikanthan, A., Pimenov, D.Y., Giasin, K. and Krishna, M. (2021). Corrosion behaviour of high-strength Al 7005 alloy and its composites reinforced with industrial waste-based fly ash and glass fibre: comparison of stir cast and extrusion conditions, Materials, 14(14), pp. 3929. DOI: 10.3390/ma14143929.
[36] Malaki, M., Tehrani, A.F., Niroumand, B., and Abdullah, A. (2021). Ultrasonically Stir Cast SiO2/A356 Metal Matrix Nanocomposites, Metals, 11(12), pp. 2004. DOI: 10.3390/met11122004.
[37] Dang, B., Jian, Z., Xu, J. and Li, S. (2017). Density and solidification shrinkage of hypereutectic Al–Si alloys, Int. J. Mater. Res., 108(10), pp. 815-819. DOI: 10.3139/146.111545.
[38] Plevachuk, Y., Egry, I., Brillo, J., Holland-Moritz, D. and Kaban, I. (2007). Density and atomic volume in liquid Al–Fe and Al–Ni binary alloys, Int. J. Mater. Res., 98(2), pp. 107-111. DOI: 10.3139/146.101447.
[39] Alaneme, K.K., Fajemisin, A.V. and Maledi, N.B. (2019). Development of aluminium-based composites reinforced with steel and graphite particles: structural, mechanical and wear characterization, J. Mater. Res. Technol., 8(1), pp. 670-682. DOI: 10.1016/j.jmrt.2018.04.019.
[40] Kumar, G.V., Rao, C.S.P. and Selvaraj, N. (2012). Studies on mechanical and dry sliding wear of Al6061–SiC composites, Compos. B. Eng., 43(3), pp. 1185-1191. DOI: 10.1016/j.compositesb.2011.08.046.
[41] Avinash, L., Ram Prabhu, T. and Bontha, S. (2016). The Effect on the dry sliding wear behavior of gravity cast A357 reinforced with dual size silicon carbide particles. In Appl. Mech. Mater., 829, pp. 83-89. DOI: 10.4028/www.scientific.net/AMM.829.83.
[42] Halil, K., İsmail, O., Sibel, D. and Ramazan, Ç. (2019). Wear and mechanical properties of Al6061/SiC/B4C hybrid composites produced with powder metallurgy, J. Mater. Res. Technol., 8(6), pp. 5348-5361. DOI: 10.1016/j.jmrt.2019.09.002.
[43] Veeresh Kumar, G.B., Pramod, R., Hari Kiran Reddy, R., Ramu, P., Kunaal Kumar, B., Madhukar, P., Chavali, M., Mohammad, F., and Khiste, S.K. (2021). Investigation of the Tribological Characteristics of Aluminum 6061-Reinforced Titanium Carbide Metal Matrix Composites. Nanomaterials, 11(11), 3039. DOI: 10.3390/nano11113039.
[44] Reddy, P.S., Kesavan, R. and Ramnath, B.V. (2018). Investigation of mechanical properties of aluminium 6061-silicon carbide, boron carbide metal matrix composite. Silicon, 10(2), pp. 495-502. DOI: 10.1007/s12633-016-9479-8.
[45] Chandla, N.K., Kant, S. Goud, M.M. (2021). Mechanical, tribological and microstructural characterization of stir cast Al-6061 metal/matrix composites—a comprehensive review. Sādhanā, 46(1), pp. 1-38. DOI: 10.1007/s12046-021-01567-7
[46] Pitchayyapillai, G., Seenikannan, P., Balasundar, P. and Narayanasamy, P. (2017). Effect of nano-silver on microstructure, mechanical and tribological properties of cast 6061 aluminum alloy, Trans. Nonferrous Met. Soc. China., 27(10), pp. 2137-2145. DOI: 10.1016/S1003-6326(17)60239-5
[47] Pitchayyapillai, G., Seenikannan, P., Raja, K. and Chandrasekaran, K. (2016). Al6061 hybrid metal matrix composite reinforced with alumina and molybdenum disulphide, Adv. Mater. Sci. Eng. DOI: 10.1155/2016/6127624.
[48] Mohammed Razzaq, A., Majid, D.L., Ishak, M.R., and Basheer, U.M. (2017). Effect of fly ash addition on the physical and mechanical properties of AA6063 alloy reinforcement, Metals, 7(11), pp. 477. DOI: 10.3390/met7110477.
[49] Sharma, S., Kini, A., Shankar, G., Rakesh, T. C., Raja, H., Chaitanya, K., & Shettar, M. (2018). Tensile fractography of artificially aged Al6061-B4C composites, J. Mech. Eng. Sci., 12(3), pp. 3866-3875. DOI: 10.15282/jmes.12.3.2018.8.0339
[50] Lakshmikanthan, A., Bontha, S., Krishna, M., Koppad, P.G. and Ramprabhu, T. (2019). Microstructure, mechanical and wear properties of the A357 composites reinforced with dual sized SiC particles, J. Alloys Compd. 786, pp. 570-580. DOI: 10.1016/j.jallcom.2019.01.382.
[51] Lakshmikanthan, A., Udayagiri, S.B., Koppad, P.G., Gupta, M., Munishamaiah, K. and Bontha, S. (2020). The effect of heat treatment on the mechanical and tribological properties of dual size SiC reinforced A357 matrix composites, J. Mater. Res. Technol. 9(3), pp. 6434-6452. DOI: 10.1016/j.jmrt.2020.04.027